TÜBİTAK

Turkish Journal of Physics

http://journals.tubitak.gov.tr/physics/

Research Article

Turk J Phys
(2013) 37: 107 – 112

doi:10.3906/fiz-1205-7

Study of zone center phonons in wolframite $ZnWO_4$

Ruby JINDAL[1], **Murari Mohan SINHA**[1,*], **Hem Chandra GUPTA**[2]
[1]Department of Physics, Sant Longowal Institute of Engineering and Technology, Longowal, Sangrur-148106, India
[2]Department of Physics, Indian Institute of Technology, Delhi Hauz Khas, New Delhi-110016, India

Received: 16.05.2012 • **Accepted:** 09.08.2012 • **Published Online:** 20.03.2013 • **Printed:** 22.04.2013

Abstract: A short-range force constant model was applied to investigate the phonons in wolframite $ZnWO_4$ crystals in their monoclinic phase having space group P2/c and symmetry C_{2h}. The normal symmetry coordinates for the monoclinic wolframite were computed. The zone center phonons were calculated by using 8 stretching and 6 bending force constants. The calculated results are in very good agreement with the observed ones. The infrared frequencies were assigned for the first time. The potential energy distribution was also investigated for determining the significance of the contribution from each force constant toward the Raman and infrared wavenumbers.

Key words: Lattice dynamics, infrared spectra, Raman spectra, zone center phonons, wolframite structure

1. Introduction

Materials belonging to the tungstate family (AWO_4) are studied because of their many practical applications. On the basis of optical and luminescence properties, these materials have wide applications as phosphors, laser host crystals, and scintillator detectors in high energy particle physics, rare-event searches, and medical diagnosis [1–4]. In particular, $ZnWO_4$, with large band gap energy, is a promising material for a new generation of radiation detectors [5].

$ZnWO_4$, also known by the mineral name sanmartinite, belongs to the divalent transition-metal tungstates of general formula AWO_4, which crystallize in either tetragonal scheelite structures or monoclinic wolframite structures depending on the size of cation A [6]. $ZnWO_4$ exhibits wolframite phases at zero and low pressure up to ~39 GPa. With an increase in pressure the fraction of the wolframite structure decreases and at about 39 GPa phase transition occurs from the wolframite structure to a monoclinic fergusonite-type structure. This monoclinic fergusonite-type phase of $ZnWO_4$ remains stable up to a pressure of 57.6 GPa. On further increase in pressure (beyond 57.6 GPa) the fergusonite-type phase of $ZnWO_4$ disappears and an orthorhombic C*mca* structure is formed [7]. According to Trots et al. [8], $ZnWO_4$ is stable in a wolframite structure and there is no occurrence of phase transition from 3 K up to 1486 K.

Vibrational studies have been used to give information about the displacements of atoms or ions, some of which are related to the polarization of the material, and Raman scattering is a useful tool for exploring the microscopic origin of the ferroelectricity of materials and to detect changes in local order involving significant variations in the anion–cation bond forces. Therefore, the Raman and infrared phonons must be studied experimentally as well as theoretically.

*Correspondence: mm_sinha@rediffmail.com

Errandonea et al. [7] studied the Raman wavenumbers in $ZnWO_4$ experimentally as well as theoretically. A few infrared modes were observed and calculated by Evarestov et al. [9] and a few were experimentally observed by Clark et al. [10]. Hence in this study an attempt was made to calculate both Raman and infrared wavenumbers theoretically using normal coordinate analysis with 8 stretching and 6 bending force constants. Very good agreement was obtained between the theoretically calculated values and the experimentally observed results. We obtained better results compared to the theoretical results obtained by Errandonea et al. [7]. The potential energy distribution was also investigated for determining the significance of the contribution from each force constant toward the Raman and infrared wavenumbers.

2. Structure

$ZnWO_4$ crystallizes in a monoclinic wolframite structure (space group symmetry P2/c = 13-C2h). The primitive cell contains 2 formula units, i.e. it contains 12 atoms in a unit cell. In the structure of wolframite $ZnWO_4$, both cations Zn and W have octahedral oxygen coordination and each octahedron shares 2 corners with its neighbors [11]. The structure is shown in the Figure. The lattice parameters are a = 4.6902(1) Å, b = 5.7169(9) Å, c = 4.9268(1) Å, $\beta = 90.62^\circ(1)$, V = 132.14(1) $Å^3$ and Z = 2 [8]. Table 1 represents the site symmetry, atomic coordinates [8], and the phonon contribution at the Γ point.

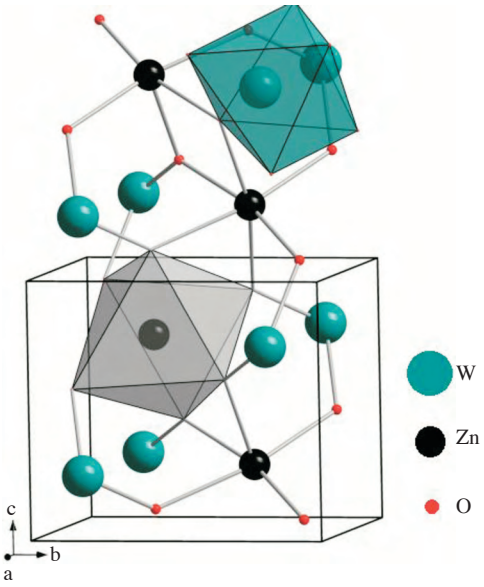

Figure. Crystal structure of $ZnWO_4$ crystals in their wolframite structure.

Table 1. Site symmetry, atomic coordinates for $ZnWO_4$, and phonon contribution at Γ point.

Atoms	Sites	X	Y	Z	Phonon contribution at point
Zn	2f	0.500	0.6838	0.250	A_g+ 2B_g+ A_u+ 2 B_u
W	2e	0.000	0.1820	0.250	A_g+ 2 B_g+ A_u+ 2 B_u
O1	4g	0.217	0.8953	0.4373	3 A_g+ 3 B_g+ 3 A_u+ 3 B_u
O2	4g	0.256	0.3747	0.3996	3 A_g+ 3 B_g+ 3 A_u+ 3 B_u

The total number of zone center phonon modes present for each species of space group is

$$\Gamma_{total} = 8Ag + 10Bg + 8Au + 10Bu$$

Out of these, 1 Au and 2 Bu are acoustical modes. Therefore, the active optical modes are given as

$$\Gamma_{optical} = 8Ag + 10Bg + 7Au + 8Bu$$

Here 8 Ag and 10 Bg are Raman active modes and 7 Au and 8 Bu are infrared active modes.

3. Theory

The determination of the frequency of normal vibrations involves the kinetic and potential energies of the system. It is necessary to solve the secular equation (containing the kinetic and potential energy matrix) to determine the normal vibrational frequency. Wilson developed the GF matrix method to solve the secular equation, which is also known as normal coordinate analysis [12]. If the potential energy matrix is represented by F and the kinetic energy matrix is represented by G^{-1}, then the secular equation can be written as

$$det|F - G^{-1}\lambda| = 0$$

In order to make the calculations easy, the above equation can also be written as

$$det|FG - E\lambda| = 0$$

where F is a matrix of force constants bringing the potential energies of vibrations into the equation. As the potential energy develops from the interaction between the atoms, so potential energy provides valuable information about the nature of interatomic forces. G is a matrix that involves the masses of the atoms and their geometrical arrangement in the molecule, bringing the kinetic energies into the equation, E is a unit matrix, and the eigenvalue λ bringing the frequency ν into the equation is defined by

$$\lambda = 4\pi^2 c^2 \nu^2$$

The matrix F was constructed by using short-range stretching force constants K_i and the bending force constants H_i. The stretching forces between 2 atoms were assumed to be obeying Hook's law [13]. Potential energies include short-range valence forces between nearest neighbors W–O1, W–O2, Zn–O1, Zn–O2, O2–O2, and W–Zn and bending forces between O1–Zn–O2, O1–W–O2, O1–W–Zn, O2–W–Zn, W–O1–W, and Zn–W–O1. The input parameters used for the calculation are the lattice parameter, masses of the atoms, symmetry coordinates, and the available Raman and infrared wavenumbers. The symmetry coordinates for the Raman and the infrared zone center modes are given in Table 2. The short-range force constants are optimized to give the best fit of the observed Raman and infrared wavenumbers. These inter-atomic force constants thus obtained are presented in Table 3.

4. Results and discussion

In this work we calculated the Raman as well as the infrared modes using the force constants, which are given in Table 3. These values are compared with the experimentally determined Raman modes by Errandonea et al. [7] and by Basiev et al. [14] in Table 4. Infrared wavenumbers calculated in the present work are compared with graphically shown values in the paper by Evarestov et al. [9]. It is clear from Table 4 that the present calculations with 8 stretching and 6 bending short-range force constants provide very good agreement with the experimental results of Raman modes. Errandonea et al. [7] also performed ab initio calculations to calculate Raman modes, which are also given in Table 4. From Table 4 it can be seen that our calculated results are

Table 2. Symmetry coordinates of $ZnWO_4$ in P2/c structure.

Species S. no. Symmetry coordinates	Species S. no. Symmetry coordinates
A_g	A_u
1. $(Zn_{1y} - Zn_{2y}) / \sqrt{2}$	19. $(Zn_{1y} + Zn_{2y}) / \sqrt{2}$
2. $(W_{1y} - W_{2y}) / \sqrt{2}$	20. $(W_{1y} + W_{2y}) / \sqrt{2}$
3. $(O1_{1X} - O1_{2X} - O1_{3X} + O1_{4X}) /2$	21. $(O1_{1X} - O1_{2X} + O1_{3X} - O1_{4X}) /2$
4. $(O1_{1Y} + O1_{2Y} - O1_{3Y} - O1_{4Y}) /2$	22. $(O1_{1Y} + O1_{2Y} + O1_{3Y} + O1_{4Y})/2$
5. $(O1_{1Z} - O1_{2Z} - O1_{3Z} + O1_{4Z}) /2$	23. $(O1_{1Z} - O1_{2Z} + O1_{3Z} - O1_{4Z}) /2$
6. $(O2_{1X} - O2_{2X} - O2_{3X} + O2_{4X}) /2$	24. $(O2_{1X} - O2_{2X} + O2_{3X} - O2_{4X}) /2$
7. $(O2_{1Y} + O2_{2Y} - O2_{3Y} - O2_{4Y})/2$	25. $(O2_{1Y} + O2_{2Y} + O2_{3Y} + O2_{4Y}) /2$
8. $(O2_{1Z} - O2_{2Z} - O2_{3Z} + O2_{4Z}) /2$	26. $(O2_{1Z} - O2_{2Z} + O2_{3Z} - O2_{4Z}) /2$
B_g	B_u
9. $(Zn_{1X} - Zn_{2X}) / \sqrt{2}$	27. $(Zn_{1X} + Zn_{2X}) / \sqrt{2}$
10. $(Zn_{1Z} - Zn_{2Z}) / \sqrt{2}$	28. $(Zn_{1Z} + Zn_{2Z}) / \sqrt{2}$
11. $(W_{1X} - W_{2X}) / \sqrt{2}$	29. $(W_{1X} + W_{2X}) / \sqrt{2}$
12. $(W_{1Z} - W_{2Z}) / \sqrt{2}$	30. $(W_{1Z} + W_{2Z}) / \sqrt{2}$
13. $(O1_{1X} + O1_{2X} - O1_{3X} - O1_{4X}) /2$	31. $(O1_{1X} + O1_{2X} + O1_{3X} + O1_{4X}) /2$
14. $(O1_{1Y} - O1_{2Y} - O1_{3Y} + O1_{4Y}) /2$	32. $(O1_{1Y} - O1_{2\ Y} + O1_{3Y} - O1_{4Y}) /2$
15. $(O1_{1Z} + O1_{2Z} - O1_{3Z} - O1_{4Z}) /2$	33. $(O1_{1Z} + O1_{2Z} + O1_{3Z} + O1_{4Z}) /2$
16. $(O2_{1X} + O2_{2X} - O2_{3X} - O2_{4X}) /2$	34. $(O2_{1X} + O2_{2X} + O2_{3X} + O2_{4X}) /2$
17. $(O2_{1Y} - O2_{2Y} - O2_{3Y} + O2_{4Y}) /2$	35. $(O2_{1Y} - O2_{2Y} + O2_{3Y} - O2_{4Y}) /2$
18. $(O2_{1Z} + O2_{2Z} - O2_{3Z} - O2_{4Z}) /2$	36. $(O2_{1Z} + O2_{2Z} + O2_{3Z} + O2_{4Z}) /2$

Table 3. Interatomic force constant values for $ZnWO_4$.

Force constant	Between atoms	Coordination number	Interatomic distance (Å)/angle*	Force constant values (N/cm)
K1	W–O2	4	1.78	3.701
K2	W–O1	4	1.90	2.073
K3	Zn–O1	4	2.02	1.102
K4	Zn–O2	4	2.08	0.643
K5	W–O1	4	2.13	0.570
K6	Zn–O2	4	2.23	0.541
K7	O2–O2	2	2.80	0.067
K8	W–Zn	4	3.68	2.495
H1	O1–Zn–O2	4	96.51	0.254
H2	O1–W–O2	4	96.92	0.123
H3	O1–W–Zn	4	26.38	0.432
H4	O2–W–Zn	4	154.78	0.016
H5	W–O1–W	4	105.93	1.690
H6	Zn–W–O1	4	62.54	0.411

*Angles are in degrees.

better than the theoretically calculated values of Raman modes reported by Errandonea et al. [7]. The potential energy distributions for each mode are investigated to determine the contribution of different force constants to various frequencies. The interpretations drawn from the PED are described below.

From theoretical calculations, the W–O1–W force constant was found to be the leading force constant for the high frequency mode, i.e 865 cm^{-1} of A_g mode, 870 cm^{-1} of B_g mode, 868 cm^{-1} of A_u mode, and 911 cm^{-1} of B_u mode.

Table 4. Calculated and observed Raman and infrared active zone centre modes (in cm^{-1}) for $ZnWO_4$.

Species	Observed wavenumbers by Errandonea et al. [7]	Observed wavenumbers by Basiev et al. [14]	Present calculated wavenumbers	Calculated wavenumbers Errandonea et al. [7]	Two dominant contributions as per PED
$A_{g,1}$	123.1	123	122	119	H2-54%, K7-12%
$A_{g,2}$	196.1	195	169	186	K3-30%, H5-28%
$A_{g,3}$	276.1	275	272	264	K4-36%, H6-22%
$A_{g,4}$	342.1	342	325	324	H6-26%, H1-18%
$A_{g,5}$	407.0	408	389	384	K8-48%, H6-17%
$A_{g,6}$	545.5	544	471	515	K2-41%, K5-14%
$A_{g,7}$	708.9	708	705	679	K1-84%, K6-5%
$A_{g,8}$	906.9	906	865	862	H5-61%, K3-15%
$B_{g,1}$	91.5	91	91	84	H2-61%, H3-12%
$B_{g,2}$	145.8	145	138	137	K6-25%, H1-20%
$B_{g,3}$	164.1	166	165	163	K5-38%, H5-19%
$B_{g,4}$	189.6	190	188	182	H6-24%, H2-21%
$B_{g,5}$	267.1	267	291	261	K4-38%, K8-19%
$B_{g,6}$	313.1	314	347	298	H6-30%, K6-17%
$B_{g,7}$	354.1	355	368	342	K8-25%, H6-20%
$B_{g,8}$	514.5	515	486	481	K2- 55%, K5-16% K1-84%, K6-5%
$B_{g,9}$	677.8	680	711	636	H5-59%, K3-16%
$B_{g,10}$	786.1	785	870	753	
A_{u1}	—		0.0		
A_{u2}	—		125		H2-56%, K7-13%
A_{u3}	—		263		K4-37%, K8-25%
A_{u4}	320		330		H6-40%, H1-21%
A_{u5}	430	450	417		K8-47%, H6-15%
A_{u6}	528	525	469		K2-46%, K5-22%
A_{u7}	628	567	704		K1-83%, K6-7%
A_{u8}	830	785	869		H5-60%, K3-15%
B_{u1}	—		0.0		
B_{u2}	—		0.0		
B_{u3}	—		95		H2-61%, H3-14%
B_{u4}	—		187		H6-35%, H2-15%
B_{u5}	—		318		K4-40%, H6-18%
B_{u6}	—		331		K4-26%, H6-23%
B_{u7}	375	353	387		K8-41%, K3-21%
B_{u8}	475	472	475		K2-44%, K5-21%
B_{u9}	710	685	711		K1-83%, K6-5%
B_{u10}	880	900	911		H5-59%, K3-13%

For frequencies 705 cm^{-1} of A_g mode, 711 cm^{-1} of B_g mode, 704 cm^{-1} of A_u mode, and 711 cm^{-1} of B_u mode, the W–O2 force constant plays an important role. Therefore, we infer that W–O stretching vibrations are very important for higher frequencies.

The internal vibrations of W atoms are dominant for frequencies 471 cm^{-1} of A_g mode, 486 cm^{-1} of B_g mode, 469 cm^{-1} of A_u mode, and 475 cm^{-1} of B_u mode.

For frequencies 389 cm^{-1} of A_g mode, 368 cm^{-1} of B_g mode, 417 cm^{-1} of A_u mode, and 387 cm^{-1} of B_u mode, the force constant W–Zn is of utmost significance. It is worth mentioning that the W–Zn bond is very important; when the calculation was done without it, the lowest frequency of B_g mode was very small compared to the experimental value.

The force constant Zn–W–O1 plays a vital role for frequencies 325 cm^{-1} of A_g mode, 347 cm^{-1} of B_g mode, 330 cm^{-1} of A_u mode, and 331 cm^{-1} of B_u mode.

From PED we arrived at the result that the Zn–O2 stretching bond is responsible for frequencies 272 cm^{-1} of A_g mode, 291 cm^{-1} of B_g mode, 263 cm^{-1} of A_u mode, and 317 cm^{-1} of B_u mode.

According to these calculations, the lower frequencies, i.e. 122 cm^{-1} of A_g mode, 91 cm^{-1} of B_g mode, 125 cm^{-1} of A_u mode, and 95 cm^{-1} of B_u mode, are dominated by the vibrations of oxygen ions (O1,O2) in the W–O plane represented by the O1–W–O2 force constant.

A precise determination of experimental infrared wavenumbers is required to further verify the present results.

References

[1] W. Chen, Y. Inagawa, T. Omatsu, M. Tateda, N. Takeuchi, Y. Usuki, *Opt. Commun.*, **194,** (2001), 401.

[2] P. Lecoq, I. Dafinei, E. Auffray, M. Scheegans, M. V. Korzhik, O. V. Missetvich, V. B. Pavlenko, A. A. Fedorov, A. N. Annenkov, V. L. Kostylev, V. D. Ligun, *Nucl. Instrum. Methods Phys. Res. A*, **365,** (1995), 291.

[3] M. Ishii and M. Kobayashi, *Prog. Cryst. Growth Charact. Mater.*, **23,** (1992), 245.

[4] D. Errandonea, F. J. Manjon, *Prog. Mater. Sci.*, **53,** (2008), 711.

[5] F. A. Danevich, V. V. Kobychev, S. S. Nagorny, D. V. Poda, V. I. Tretyak, S. S. Yurchenko, Y. G. Zdesenko, *Nucl. Instrum., Methods Phys. Res. A*, **544,** (2005), 553.

[6] A. W. Sleight, Acta Crystallogr., Sect. B: *Struct. Crystallogr. Cryst. Chem.*, **28,** (1972), 2899.

[7] D. Errandonea, F. J. Manjon, N. Garro, P. Rodriguez-Hernandez, S. Radescu, A. Mujica, A. Muñoz, C. Y. Tu, *Phys. Rev. B*, **78,** (2008), 054116.

[8] D. M. Trots, A. Senyshyn, L. Vasylechko, R. Niewa, T. Vad, V. B. Mikhailik, H. Kraus, *J. Phys. Condens. Matter*, **21,** (2009), 325402.

[9] R. A. Evarestov, A. Kalinko, A. Kuzmin, M. Losev, J. Purans, *Integrated Ferroelectrics*, **108,** (2009), 1.

[10] G. M. Clark, W. P. Doyle, *Spectrochim. Acta.* **22,** (1966), 1441.

[11] R. O. Keeling, *Acta Crystallogr*, **10,** (1957), 209.

[12] T. Shimanouchi, M. Tsuboi, T. Miyazawa, *J. Chem. Phys.*, **35,** (1961), 1597.

[13] H. C. Gupta, Archana, Vandna Luthra, *Journal of Molecular Structure*, **984,** (2010), 204.

[14] T. T. Basiev, A. Ya. Karasik, A. A. Sobol, D. S. Chunaev, V. E. Shukshin, *Quantum Electronics*, **41,** (2011), 370.